Cooperative self-association of phosphorylase kinase from rabbit skeletal muscle

ARTICLE · JANUARY 2008

CITATIONS
2

READS
19

5 AUTHORS, INCLUDING:

Natalia A Chebotareva
Russian Academy of Sciences
115 PUBLICATIONS **1,176** CITATIONS
SEE PROFILE

Boris Kurganov
Russian Academy of Sciences
342 PUBLICATIONS **3,106** CITATIONS
SEE PROFILE

ELSEVIER

Biophysical Chemistry 133 (2008) 45–53

Biophysical Chemistry

http://www.elsevier.com/locate/biophyschem

Cooperative self-association of phosphorylase kinase from rabbit skeletal muscle

Natalia A. Chebotareva *, Alexey V. Meremyanin, Valentina F. Makeeva, Natalia B. Livanova, Boris I. Kurganov

Bach Institute of Biochemistry, Russian Academy of Sciences, Leninsky 33, Moscow, 119071, Russia

Received 22 October 2007; received in revised form 3 December 2007; accepted 4 December 2007
Available online 14 December 2007

Abstract

Ca^{2+}- and Mg^{2+}-induced association of phosphorylase kinase (PhK) from rabbit skeletal muscle has been studied at the magnitudes of the ionic strength close to the physiological values (40 mM Hepes, pH 6.8, containing 0.1 M NaCl, 0.1 mM Ca^{2+}, 10 mM Mg^{2+}; 25 °C) and under the molecular crowding conditions produced by high concentrations (1 M) of the natural osmolyte, trimethylamine N-oxide (TMAO). In the presence of 0.1 M NaCl two forms of PhK were registered, namely the "basic form" and "highly associated form", suggesting that PhK association may be treated as an example of cooperative association. According to the data on dynamic light scattering the average hydrodynamic radii of these forms were 16 and 144 nm. The addition of 1 M TMAO produces the time dependent increase in the light scattering intensity caused by the conversion of the basic form into the highly associated form. According to the data of the sedimentation analysis the basic form of PhK comprises a hexadecamer (M_r=1320 kDa) and its small associates. The removal of Ca^{2+} by addition of EGTA results in the reverse conversion of the highly associated form into the basic form suggesting reversibility of self-association of PhK. FAD, the ligand that is specifically bound to PhK, blocks the conversion of the basic form of PhK into the highly associated form.

Keywords: Phosphorylase kinase; Self-association; Crowding; TMAO; DLS; Sedimentation velocity

1. Introduction

Phosphorylase kinase (PhK; EC 2.7.1.38) catalyzing phosphorylation and activation of glycogen phosphorylase *b* (Ph*b*) plays a key role in the cascade system of regulation of glycogen metabolism [1–3]. The PhK molecule is a hexadecamer with the subunit composition $(\alpha\beta\gamma\delta)_4$ and molecular mass of 1320 kDa [4]. Ca^{2+} is the obligatory allosteric activator of PhK. It binds to an integral, nondissociable molecule of calmodulin (δ-subunit), and thus reveals the protein kinase activity of the catalytic γ-subunit [5], which in the absence of Ca^{2+} ions is constrained by the regulatory α- and β-subunits. The changes in the secondary and tertiary structure of PhK after Ca^{2+} ions binding are modest, whereas the electrostatic changes, induced by this allosteric activator, are noticeable [6]. Probably, mainly these electrostatic changes cause the transformation of PhK on the level of quaternary structure and supramolecular complexes formation. The oligomeric state of the native enzyme is strongly dependent on the protein, Ca^{2+}, and Mg^{2+} concentrations [7–10]. In muscle cells phosporylase kinase is found in two different compartments: a major fraction of the enzyme is present in the cytosol preferentially associated with the protein-glycogen particles; a minor fraction is bound to the sarcoplasmic reticulum membrane [11].

Most living cells adapt to environmental stress (osmotic, thermal, or chemical) by accumulating intracellular osmolytes. Osmolytes are small organic molecules, such as polyols, certain amino acids, and methylamines. They protect proteins under stress conditions [12–16] and regulate a cell volume [17]. For example, the tissues of sharks and rays contain urea in high

Abbreviations: PhK, phosphorylase kinase; TMAO, trimethylamine N-oxide; DLS, dynamic light scattering.

* Corresponding author. Tel.: +7 495 952 5641; fax: +7 495 954 2732.
E-mail address: chebotareva@inbi.ras.ru (N.A. Chebotareva).

0301-4622/$ - see front matter © 2007 Elsevier B.V. All rights reserved.
doi:10.1016/j.bpc.2007.12.001

concentration. It is well known, that urea causes denaturation of the proteins, but this effect could be compensated through supporting the high concentration of the counteracting osmolytes, especially trimethylamine N-oxide (TMAO), betaine, and sarcosine [12–18].

The salts of ocean water (mainly NaCl) yield an average osmotic concentration of ~1000 mOsm/l [17]. To prevent osmotic shrinkage, internal fluids of marine osmoconformers have about the same osmotic pressure as their environment (e.g. 1000 mOsm) [17]. TMAO has been shown to counteract *in vivo* the damaging effects of urea [18,19], salts and hydrostatic pressure [20] on proteins in deep-sea animals.

It was shown *in vitro* that TMAO favors protein association and formation of supramolecular structures. For example, TMAO promotes assembly and bundling of the bacterial cell division protein (FtsZ) and counteracts the denaturing effects of urea [21]. TMAO was also found to stimulate tubulin polymerization [22]. At 1 M TMAO, tubulin polymers are produced with properties expected of normal steady-state microtubules. At 2 M TMAO, polymerization is very rapid and hyperstable polymers are formed. TMAO did not interfere with binding of microtubules-associated proteins and protected tubulin assembly from urea [22]. Yang et al. [23] showed that TMAO accelerates the main steps in the amyloidal pathway (early nucleation, conformational changes, and also the protofibril–fibril transformation).

We previously demonstrated the effect of high concentrations of TMAO on self-association of glycogen phosphorylase *b* (from rabbit skeletal muscle) induced by 1 mM AMP [24]. In the presence of 1 M TMAO, the association constant for dimer–tetramer equilibrium increases 2-fold. However the effect of excluded volume on the dimer–tetramer equilibrium is compensated by the shift of equilibrium in the isomerization reaction of the dimer T↔R towards the more compact, non-associating T-conformation [24].

TMAO is almost neutral (zwitterionic form) in the pH range 6.0–8.0. It has pK_a in the range 4.56–4.75 [25,26]. Singh and colleagues [27] investigated thermal denaturation of three model proteins, namely, pancreatic RNase A, hen egg white lysozyme, and bovine apo-α-lactalbumin in the pH range 2.0–7.0. It has been shown that positively charged form of TMAO (at pH < pK_a) destabilizes all proteins, whereas zwitterionic form of TMAO (at pH > pK_a) stabilizes proteins. The authors consider that zwitterionic form of TMAO is excluded from the protein surface at pH > pK_a, while positively charged form binds to proteins at pH values below pK_a [27].

It should be noted that some authors interpret the effect of osmolytes on biochemical systems in terms of statistical mechanics using the theory of excluded volume (crowding), and calculating the second virial coefficients, which characterize the interactions of the molecules in solution [28–39]. Other researchers operate with the terms of preferential hydration of the protein and the free energy [40–46]. Winzor and Wills [14,15,28] and Davies-Searle et al. [31] analyzed both approaches and showed that the results they give are practically equivalent.

To reveal the molecular mechanisms underlying the effects of crowding on the intracellular biochemical processes, we used high concentrations of osmolytes that mimic the crowding conditions. Previously we showed that high concentrations of TMAO favor self-association of PhK at low ionic strength in the presence of Ca^{2+} ions [47–49]. Such an enhancement of PhK association was interpreted as an effect of crowding arising from the presence of high concentrations of the cosolvent. In the present work we studied self-association of PhK using dynamic light scattering (DLS) and analytical ultracentrifugation at the physiological ionic strength and in the presence of 1 M TMAO, i.e., under the conditions simulating molecular crowding in the cell. It has been shown that under these conditions the facilitation of PhK association induced by the crowding-agent is due purely to cooperative conversion of the basic form of PhK (the original hexadecameric form) into the highly associated form including hundreds of the PhK molecules.

2. Materials and methods

2.1. Materials

TMAO, Hepes, FAD, and EGTA were purchased from Sigma Chemical Co. (USA). DEAE-Toyopearl 650 M was purchased from Tosoh (Japan). The reagents were used without additional purification. When preparing the samples containing TMAO, the initial pH of osmolyte solution in 40 mM Hepes buffer was adjusted so that the final pH was 6.8. The dynamic viscosity of TMAO solutions was measured using Anton Paar viscosimeter at 25 °C.

2.2. Isolation and purification of PhK

PhK was isolated from rabbit skeletal muscle according to Cohen [4] using ion-exchange chromatography on DEAE-Toyopearl 650 M as a final step of purification [50]. The purity of enzyme was confirmed by SDS-PAGE electrophoresis [51]. Preparations of PhK in 25 mM Na-glycerol β-phosphate buffer, pH 7.05, containing 1 mM EDTA, 0.5 mM 2-mercaptoetanol, and 50% glycerol were stored for 3 weeks at −20 °C. Before the experiments PhK was dialyzed against 40 mM Hepes buffer, pH 6.8, at 4 °C. The PhK concentration was determined spectrophotometrically at 280 nm using the absorption coefficient 1.24 cm^2 mg^{-1} [4].

2.3. DLS studies

For light scattering measurements a commercial instrument Photocor Complex was used (Photocor Instruments Inc., USA; www.photocor.com). A He–Ne laser (Coherent, USA, Model 31-2082, 632.8 nm, 10 mW) has been used as a light source. The temperature of sample cell was controlled by the proportional integral derivative (PID) temperature controller to within ±0.1 °C. The quasi-cross correlation photon counting system with two photomultiplier tubes (PMT) was used to increase the accuracy of particle sizing in the range of 0.5–5000 nm. DLS data have been accumulated and analyzed with multifunctional real-time correlator Photocor-FC using both logarithmic multiple-tau and linear time-scale modes. DynaLS software (Alango, Israel) was used for polydisperse analysis of DLS data.

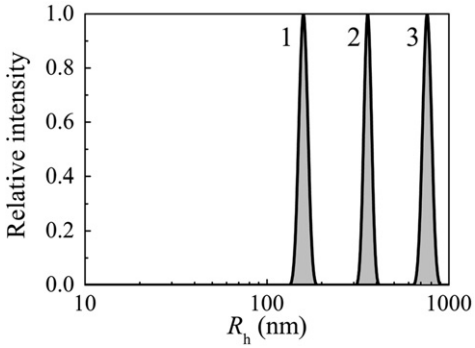

Fig. 1. Analysis of association of PhK (0.2 mg/mL) by DLS at 25 °C (40 mM Hepes buffer, pH 6.8, containing 0.1 mM Ca^{2+}, 10 mM Mg^{2+}). Distribution of the particles by their size registered at various times of incubation: (1) 2, (2) 5, and (3) 25 min. Association of PhK was initiated by the addition of Ca^{2+} and Mg^{2+} to the enzyme solution. DLS measurements were carried out at a scattering angle of 90°.

The kinetics of self-association of PhK were studied by DLS in 40 mM Hepes buffer, pH 6.8. All solutions for the experiments were prepared using deionized water obtained with Easy-Pure II RF system (Barnstead, USA). The buffer was placed in a cylindrical cell with the internal diameter of 6.3 mm and preincubated for 5 min at 25 °C. The association process was initiated by the addition of an aliquot of PhK (or Ca^{2+} and Mg^{2+}) solution to the final volume of 0.5 mL. When studying the kinetics of self-association of PhK, the scattering light was collected at 90° scattering angle.

Dynamic light scattering may be correctly employed for determination of average current size of particles, provided that characteristic aggregation time was much higher than the time required for measurement of each size particle. In our experiments the accumulation time of the autocorrelation function was 30 s. Such a selection of the accumulation time allows the reliable construction of the autocorrelation function to be carried out in the case when time-dependent association of the PhK molecules takes place. To characterize the broadness of the distribution of particles by size, we used the dimensionless polydispersity index PI: $PI=\mu_2/\bar{\Gamma}^2$, where $\bar{\Gamma}$ is the average decay rate of the autocorrelation function and μ_2 is the second cumulant (see ISO standard [52]).

2.4. Analytical ultracentrifugation

Sedimentation velocity experiments were carried out in a Model E analytical ultracentrifuge (Beckman), equipped with absorbance optics, a photoelectric scanner, a monochromator, and a computer on line. A four-hole rotor An–F Ti and 12 mm double sector cells were used. Sedimentation profiles were recorded by measuring the enzyme absorbance at 280 nm. All cells were scanned simultaneously. The time interval between scans was 3 min. For digital data acquisitions La-n20-12 PC1 and La-1.5 PCI plates and software specially written by A.G. Zharov (www.ADClab.ru) were used. The sedimentation coefficients were estimated from a differential sedimentation coefficient and frictional ratio distribution [$c(s, f/f_0)$ versus s] and a general sedimentation coefficient distribution $c(s,*)$ using SEDFIT program [53,54]. The $c(s, f/f_0)$ analysis was performed with regularization at confidence levels of 0.68 and 0.95. The sedimentation coefficients were corrected to solvent density and viscosity (20 °C, water) in the standard way [55].

Origin 7.0 software (OriginLab Corporation, USA) was used for the calculations.

3. Results

3.1. Effect of Ionic Strength on PhK Self-Association

Ca^{2+}- and Mg^{2+}-induced association of PhK was analyzed in 40 mM Hepes, pH 6.8, by measuring the size of the particles formed in the course of protein self-association. The distributions of particles by size registered by DLS at various times of incubation of PhK with 0.1 mM Ca^{2+} and 10 mM Mg^{2+} were unimodal, with higher mean hydrodynamic radii (R_h) of the associates at longer incubation times (Fig. 1). The polydispersity index PI characterizing the broadness of the distribution function remained constant at variation of the incubation time and was found to be 0.35±0.02.

Fig. 2A and B show time dependences of the light scattering intensity and hydrodynamic radius. When interpreting the

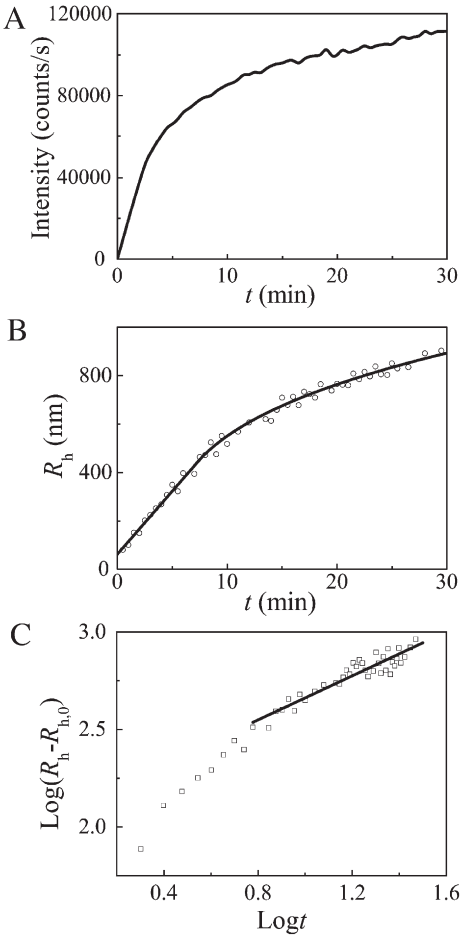

Fig. 2. Kinetics of association of PhK (0.2 mg/mL) in 40 mM Hepes buffer, pH 6.8, containing 0.1 mM Ca^{2+}, 10 mM Mg^{2+}. Dependences of the light scattering intensity and the hydrodynamic radius (R_h) on time (A and B, respectively). (C) Dependence of R_h on time in the logarithmic coordinates. Dimensions of R_h and t are nm and min, respectively.

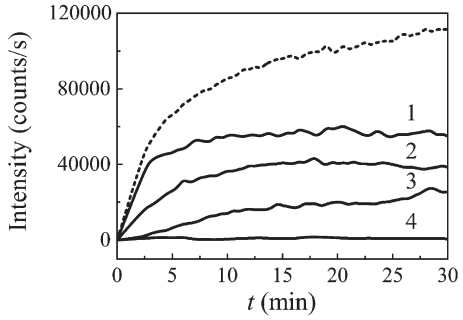

Fig. 3. Effect of NaCl on the kinetics of association of PhK (0.2 mg/mL). The dependences of the light scattering intensity on time in the absence (dashed line) and presence of various concentrations of NaCl: (1) 5, (2) 10, (3) 15, and 100 mM (4).

character of the dependence of hydrodynamic radius on time, the following considerations should be taken into account. Namely, the hydrodynamic radius of the PhK hexadecamer measured in the absence of Ca^{2+} and Mg^{2+} was found to be 13.0±0.5 nm. The initial part of the dependence of R_h on time obtained for Ca^{2+}- and Mg^{2+}-induced association of PhK is linear (Fig. 2B). The extrapolation of the R_h value to the initial instant of time gives the value of 78±1 nm. Let designate this value as $R_{h,0}$. Thus, the initial stage of self-association of PhK represents the formation of the start associates with $R_{h,0}$=78 nm. Further sticking of the start associates (and associates of higher order) results eventually in the formation of even larger associates with $R_h \approx 900$ nm. The dependence of Log ($R_h - R_{h,0}$) on Log t approaches a straight line with the slope of 0.56±0.03 at high values of the time (Fig. 2C). Thus, the R_h value is proportional to $t^{0.56}$ at $t \to \infty$.

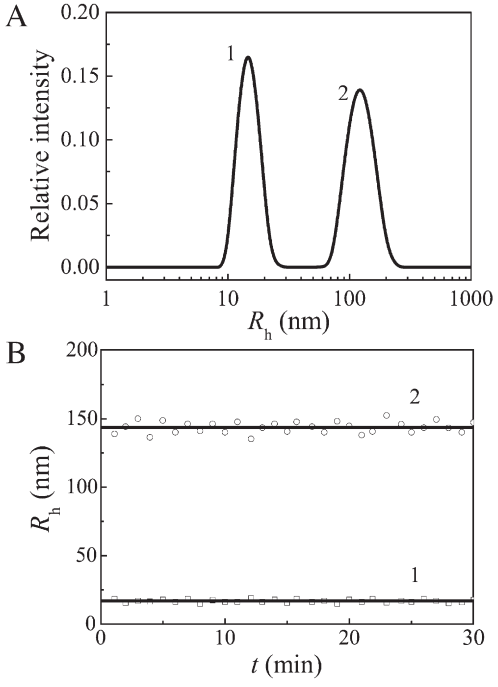

Fig. 4. Association of PhK (0.2 mg/mL) in the presence of 100 mM NaCl. (A) Distribution of the particles by their size. (B) Dependences of the R_h values for the basic and highly associated forms (1 and 2, respectively) on time.

The study of the effect of ionic strength on the kinetics of PhK self-association shows that high concentrations of NaCl suppress the increment of the light scattering intensity after the addition of Ca^{2+} and Mg^{2+} to the enzyme solution (Fig. 3). When the concentration of NaCl was 100 mM, the effect of suppression was complete (curve 4 in Fig. 3).

To characterize the size of the enzyme forms existing in the buffer containing 100 mM NaCl, we measured the distribution of the particles by their size. Two forms of PhK associates were detected (Fig. 4A). The size of each form remained unchangeable during incubation. The average value of the hydrodynamic radius of the particles of the lesser size was 16±1 nm (line 1 in Fig. 4B). Thus, the size of these particles is close to that for the original PhK hexadecamer. Therefore this form of PhK was denoted "the basic form". The average value of the hydrodynamic radius of the particles of the larger size was 144±2 nm (line 2 in Fig. 4B). This

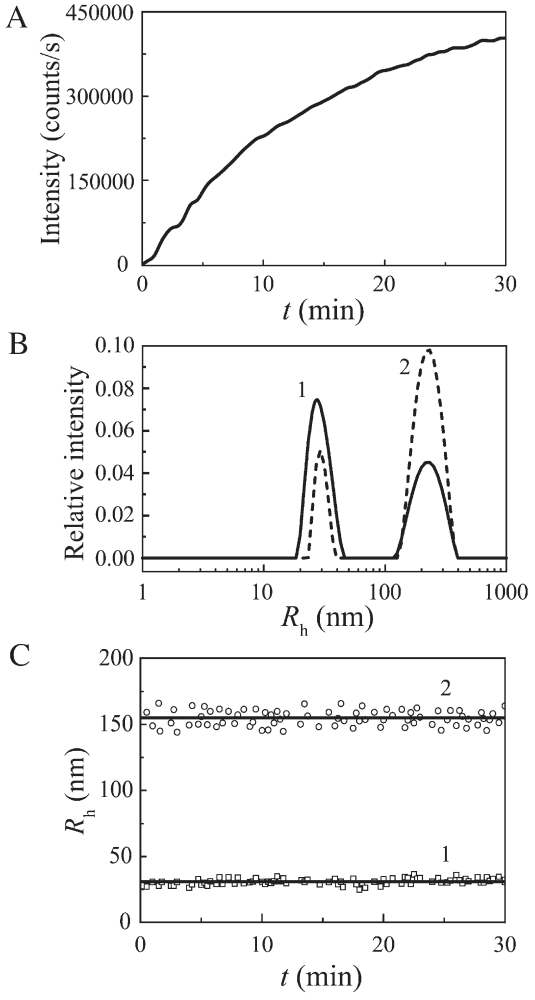

Fig. 5. Kinetics of self-association of PhK (0.2 mg/ml) in 40 mM Hepes buffer, pH 6.8, containing 0.1 M NaCl under molecular crowding conditions arising from the presence of 1 M TMAO. (A) Dependence of the light scattering intensity on time. Association of PhK was initiated by the addition of the enzyme to the buffer solution, containing 0.1 M NaCl, 0.1 mM Ca^{2+}, 10 mM Mg^{2+}, and 1 M TMAO. (B) Distribution of the particles by their size. Time of incubation: 1 and 12 min (solid and dotted curves, respectively). (C) Dependences of the R_h value for the basic (1) and highly associated (2) forms on time.

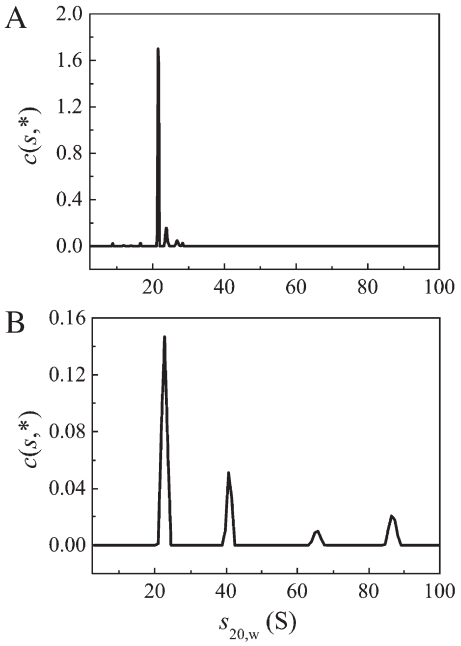

Fig. 6. Sedimentation behavior of PhK (0.2 mg/mL) at high rotor speed (30000 rpm) at 20 °C in 40 mM Hepes buffer, pH 6.8, containing 0.1 M NaCl, 0.1 mM Ca^{2+}, 10 mM Mg^{2+}. Differential sedimentation coefficient distributions $c(s, f/f_0)$ for PhK were obtained in the absence (A) and presence of TMAO (B). Sedimentation coefficient distributions were corrected to the standard conditions and saved as one-dimensional $c(s,*)$ distributions.

form was called "the highly associated form". It should be noted that the "highly associated form" is really a polydisperse set of the particles of the closely related sizes.

3.2. Effect of TMAO on self-association of PhK

Although 100 mM NaCl suppresses completely the kinetics of self-association of PhK, 1 M TMAO appeared to cause the increase in the light scattering intensity of the PhK solution (Fig. 5A). The measurement of the distribution of the particles by their size allowed us to make a conclusion about the reason of the enhancement of the light scattering intensity. It turned out that the system contained the particles of two sizes (Fig. 5B). The average values of the hydrodynamic radius for these forms of PhK remained unchangeable in time (31±2 and 155±3 nm; Fig. 5C) and close to those for the basic and highly associated forms registered in the absence of 1 M TMAO (cf. Fig. 4B).

The portion of the basic form decreases with time, whereas the portion of the highly associated form tends to increase. Thus, the increase in the light scattering intensity of the PhK solution after the addition of the crowding-agent (1 M TMAO) is due to the conversion of the basic form of PhK into the highly associated form.

3.3. Characterization of the basic form of PhK by analytical ultracentrifugation

Sedimentation velocity was used to characterize in more detail the basic form of PhK. As for the highly associated form its size is too large to be studied by analytical ultracentrifugation.

Fig. 6 shows sedimentation behavior of PhK (0.2 mg/mL) at high rotor speed (30000 rpm). At selected rotor speed the highly associated form of PhK is completely precipitated before the attainment of the given speed. Thus, such an experiment allows us to characterize the basic form of PhK. In the absence of TMAO the main peak corresponds to the hexadecameric form of PhK ($s_{20,w}$=21.5±0.2 S; Fig. 6A). As seen from Fig. 6B, under molecular crowding conditions arising from the presence of 1 M TMAO there are four peaks with the sedimentation coefficients of 22.7±0.5, 40.8±0.4, 65.5±0.6, 86.8±0.7 S. These peaks correspond to the hexadecameric form of PhK and its small associates, containing from 2 to 8 hexadecamers. A small difference between sedimentation coefficient values of a hexadecamer in the absence (21.5±0.2 S) and in the presence of 1 M TMAO (22.7±0.5 S) may be explained by more compact conformation of the PhK molecule under crowding conditions. It is worth noting that according to molecular crowding theory the compact states of macromolecules are favored over asymmetric ones [56].

The estimation of the size of the basic form of PhK in the presence of 1 M TMAO allows us to compare the resolution of DLS and sedimentation velocity method. The distribution of particles by size obtained by DLS is unimodal, whereas four peaks are seen on the differential sedimentation coefficient distribution $c(s, f/f_0)$. These results indicate that sedimentation velocity is characterized by higher resolution than DLS.

When comparing the values of the hydrodynamic radius of the basic form obtained in the absence and presence of 1 M

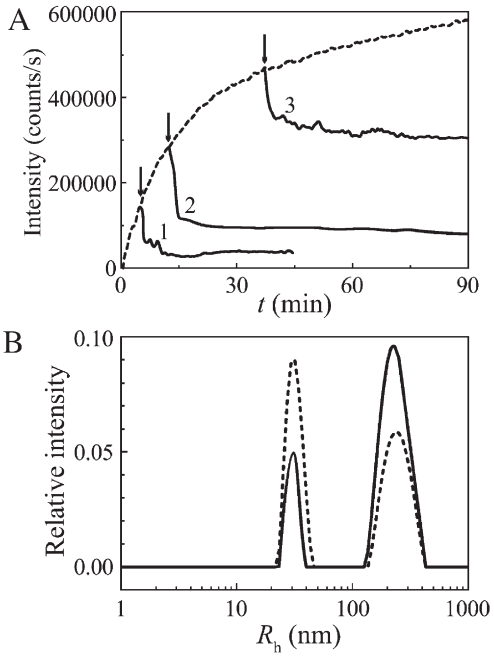

Fig. 7. The effect of EGTA (1 mM) on self-association of PhK (0.2 mg/ml) under molecular crowding conditions arising from the presence of 1 M TMAO (40 mM Hepes buffer, pH 6.8, containing 0.1 M NaCl). (A) Dependences of the light scattering intensity on time obtained in the absence of EGTA (the dotted line) and after the addition of EGTA. Arrows show the points in time at which EGTA was added: (1) 5, (2) 12, and (3) 37 min. (B) Distribution of the particles by their size registered after 12 min incubation before the addition of EGTA (solid curve) and after further 78 min incubation with 1 mM EGTA (dotted curve).

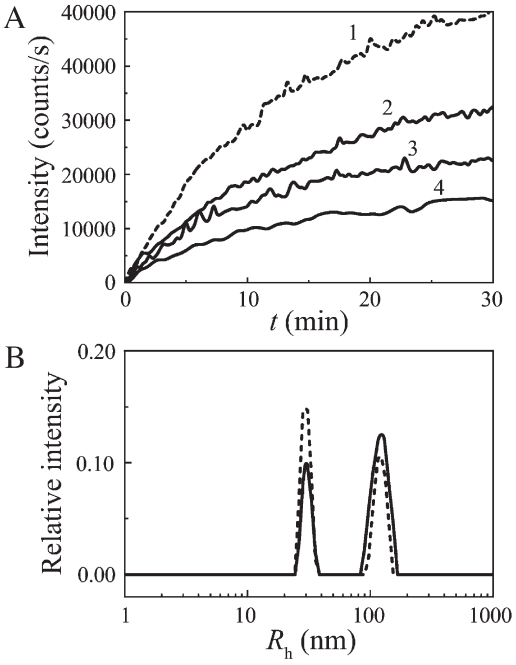

Fig. 8. The effect of FAD on the self-association of PhK (0.2 mg/mL) under molecular crowding conditions. (A) The dependences of the light scattering intensity on time obtained in the absence (1) and presence of FAD at the following concentrations: (2) 5, (3) 30, and 60 (4) μM. (B) Distributions of the particles by their size registered after 30 min incubation in the absence and presence of 60 μM FAD (solid and dotted curves, respectively).

TMAO (16±1 and 31±2 nm, respectively), we should take into account that according to the sedimentation velocity data the basic form in the latter case contains hexadecamer and higher associates of 2 to 8 hexadecamers.

It has been just the presence of small associates which results in the increase in the average R_h value for the basic form under molecular crowding conditions.

3.4. Reversibility of PhK self-association

To check the reversibility of self-association of PhK under the molecular crowding conditions, the Ca^{2+}-binding agent, EGTA, was added at definite intervals after the initiation of PhK association. Fig. 7A shows the effect of EGTA added within 5, 12, and 37 min of the onset of the reaction. The addition of 1 mM EGTA ceases the increase in the light scattering intensity (I) and results in the abrupt decrease in the I value. For example, curve 2 in Fig. 7A shows the decrease in the light scattering intensity after the addition of 1 mM EGTA at t=12 min. The measurement of the distribution of the particles by their size allowed us to elucidate the reason of such a decrease in the I value. Fig. 7B shows the distribution of the particles by their size registered after 12 min incubation before the addition of EGTA (solid curve) and after further 78 min incubation with 1 mM EGTA (dotted curve). On the basis of these data one can conclude that the removal of Ca^{2+} results in the reverse conversion of the highly associated form into the basic form of PhK. Thus, self-association of PhK under molecular crowding conditions arising from the presence of 1 M TMAO is a reversible process.

3.5. Effect of FAD on PhK self-association

Previously [57] using analytical ultracentrifugation we have shown that PhK is capable of binding FAD. Besides, FAD inhibits the formation of PhK-glycogen complex. These facts are indicative of the presence of the FAD-binding sites in the PhK molecule. It was of interest to study the effect of FAD on self-association of PhK under the crowding conditions. As seen from Fig. 8A, FAD suppresses the enhancement of the light scattering intensity accompanying PhK self-association. The comparison of the distribution of the particles by their size registered after 30 min incubation in the absence and presence of 60 μM FAD (solid and dotted curves, respectively, in Fig. 8B) indicates that the suppression of PhK self-association under the action of FAD is due to blocking the conversion of the basic form of PhK into the highly-associated form.

The analysis of basic form of PhK in the presence of 10 μM of FAD (0,1 M NaCl and 1 M TMAO) by sedimentation velocity showed that the $c(s, f/f_0)$ distribution has the same set of peaks as in the absence of FAD (data not shown).

4. Discussion

It has been shown in the present work that at low ionic strength Ca^{2+}- and Mg^{2+}-induced association of PhK proceeds through the stage of the formation of the start associates with $R_{h,0}$=78 nm. The fact that the limiting slope of the dependence of Log ($R_h - R_{h,0}$) on Log t is equal to 0.56 at long incubation time is indicative of the fulfillment of the power function for the dependence of R_h on time, i.e., $R_h \sim t^{0.56}$. It should be noted that the kinetics of self-association of PhK are analogous to those for irreversible thermal aggregation of protein. Using dynamic light scattering we showed that the first stage of protein thermal aggregation is the formation of the start aggregates [58–62]. For example, in the case of thermal aggregation of glyceraldehyde 3-phosphate dehydrogenase from rabbit skeletal muscle the hydrodynamic radius of the start aggregates was found to be 21 nm [60]. The initial part of the dependence of the hydrodynamic radius of the protein aggregates on time is linear. At high values of time the dependence of R_h on time follows the power function: $R_h \sim t^{1/1.8}$. According to the theory of colloid aggregation [63–68] these results imply that sticking of the start aggregates and aggregates of higher order proceeds in the kinetic regime wherein the rate of aggregation is limited by diffusion of the interacting particles (each collision of the interacting particles results in their sticking together). This regime of aggregation is called “diffusion-limited cluster–cluster aggregation” (DLCA). For DLCA regime of aggregation the dependence of R_h on time at long incubation is described by the power function: $R_h \sim t^{1/d_f}$, where d_f is the fractal dimension of aggregates. DLCA regime is characterized by the universal value of d_f, namely d_f=1.8. Thus, the R_h should be proportional to $t^{1/1.8}=t^{0.56}$. It is precisely this power function for the dependence of R_h on time that was observed in the case of self-association of PhK at low ionic strength. The similarity of the kinetics of PhK self-association at low ionic strength to the kinetics of thermal aggregation of proteins allows us to conclude the association of PhK under conditions studied proceeds in DLCA regime.

It should be noted that aggregates which are formed in the DLCA regime are characterized by narrow distribution of particles by size [63]. We observed such narrow distributions of particles by size for thermal aggregation of a number of proteins: rabbit muscle glycogen phosphorylase *b* [58], β_L-crystallin from bovine lens [59], and rabbit muscle glyceraldehyde-3-phosphate dehydrogenase [60]. Thus, it is not surprising that distributions of particles by size for PhK associates formed at low ionic strength (Fig. 1) look like well defined peaks.

At rather high value of ionic strength, namely in 0.1 M NaCl, association of PhK comes to a halt on the stage of the formation of the highly associated form with $R_h = 144$ nm. One can assume that high ionic strength suppresses further association of this form. Thus, the existence of the basic and highly associated forms of PhK in 0.1 M NaCl may be treated as a cooperative association of PhK. The term "cooperative association" was proposed for the case of association of biological macromolecules resulting in the formation of the highly associated form without the accumulation of the intermediate forms in appreciable amounts [69,70]. In other words, in the case of cooperative association only monomer and highly associated form exist in the system. Such a situation was demonstrated experimentally for hemerythrin. Octameric molecule of hemerythrin is in mobile equilibrium with monomeric subunits [71]. The enzymatic properties of the associating protein systems of the type monomer ⇄ *N*-mer and the binding of specific ligands in these systems were discussed in the theoretical works [72–74]. From this viewpoint PhK may be considered as slowly associating enzyme system of the monomer ⇄ *N*-mer type.

In the present work we have demonstrated that under crowding conditions arising from the presence of 1 M TMAO the basic form of PhK is converted into the highly associated form. This result is in good agreement with the idea that crowding favors the formation of compact protein associates.

We showed that self-association of PhK under crowding conditions is a reversible, Ca^{2+}-dependent process. The removal of Ca^{2+} results in the reverse conversion of the highly associated form into the basic form of PhK.

It is possible to speculate that the physiological significance of the existence of the highly associated form of PhK in the presence of Ca^{2+} under crowding conditions may be connected with the formation of the depot form of the enzyme providing the increase in stability and, consequently, the lifetime of PhK in the cell. The interconversion between the basic and highly associated forms of PhK may be under the control of cellular metabolites. Among such metabolites is FAD. This metabolite is of special interest because enzymes of protein–glycogen particles have affinity to flavins. This was demonstrated for glycogen phosphorylase [75,76], glycogen synthase [77], and PhK [57], suggesting that protein–glycogen particles may function as a flavin depot. Taking into account the ability of FAD to prevent the formation of the PhK-glycogen complex [57], one can assume that FAD controls localization and aggregation state of PhK.

Acknowledgements

We thank Dr. I.E. Andreeva for critical reading of the manuscript and helpful discussion. This research was supported by the Russian Foundation for Basic Research (grants 08-04-00666-a and 06-04-39008), Program "Molecular and Cell Biology" of the Presidium of the Russian Academy of Sciences.

References

[1] E.G. Krebs, D.J. Graves, E.H. Fisher, Factors affecting the activity of muscle phosphorylase *b* kinase, J. Biol. Chem. 23 (1959) 2867–2873.
[2] R.J. Brusharia, D.A. Walsh, Phosphorylase kinase: the complexity of its regulation is reflected in the complexity of its structure, Frontiers Biosci. 4 (1999) 618–641.
[3] N.B. Livanova, Structure and regulation of the activity of muscle phosphorylase kinase, Biochemistry (Moscow) 58 (1993) 1677–1684.
[4] P. Cohen, The subunit structure of rabbit skeletal muscle phosphorylase kinase, and the molecular basis of its activation reactions, Eur. J. Biochem. 34 (1973) 1–14.
[5] K.-F.J. Chan, D.J. Graves, Rabbit skeletal muscle phosphorylase kinase. Catalytic and regulatory properties of the active αγδ and γδ complexes, J. Biol. Chem. 257 (1982) 5948–5955.
[6] T.S. Priddy, C.R. Middaugh, G.M. Carlson, Electrostatic changes in phosphorylase kinase induced by its obligatory allosteric activator Ca^{2+}, Protein Sci. 16 (2007) 517–527.
[7] D.A. Wilkinson, T.J. Fitzgerald, T.N. Marion, G.M. Carlson, Mg^{2+} induces conformational changes in the catalytic subunit of phosphorylase kinase, whether by itself or as part of the holoenzyme complex, J. Protein. Chem. 18 (1999) 157–164.
[8] O.W. Nadeaw, G.M. Carlson, E.P. Gogol, Ca^{2+}-dependent global conformational change in 3D structure of phosphorylase kinase obtained from electron microscopy, Structure 10 (2002) 23–32.
[9] T.S. Priddy, B.A. MacDonald, W.T. Heller, O.W. Nadeau, J. Trewhella, G.M. Carlson, Ca^{2+}-induced structural changes in phosphorylase kinase detected by small-angle X-ray scattering, Protein Sci. 14 (2005) 1039–1048.
[10] T.S. Priddy, E.S. Price, C.K. Johnson, G.M. Carlson, Single molecule analyses of the conformational substates of calmodulin bound to the phosphorylase kinase complex, Protein Sci. 16 (2007) 1017–1023.
[11] S.V. Polishchuk, N.R. Brandt, H.E. Meyer, M. Varsanyi, L.M.G. Heilmeyer Jr., Does phosphorylase kinase control glycogen biosynthesis in skeletal muscle? FEBS Lett. 362 (1995) 271–275.
[12] P.H. Yancey, G.N. Somero, Counteraction of urea destabilization of protein structure by methylamine osmoregulatory compounds of elasmobranch fishes, Biochem J. 183 (1979) 317–323.
[13] P.H. Yancey, M.E. Clark, S.C. Hand, R.D. Bowlus, G.N. Somero, Living with water stress: Evolution of osmolytes systems, Science 217 (1982) 1214–1222.
[14] A. Wang, D.W. Bolen, A naturally occurring protective system in urea-rich cells: mechanism of osmolyte protection of proteins against urea denaturation, Biochemistry 36 (1997) 9101–9108.
[15] D.W. Bolen, I.V. Baskakov, The osmofobic effect: natural selection of a thermodynamic force in protein folding, J. Mol. Biol. 310 (2001) 955–963.
[16] M.B. Burg, E.M. Peters, Urea and methylamines have similar effects on aldosereductase activity, Am. J. Physiology 273 (1997) 1048–1053.
[17] P.H. Yancey, Organic osmolytes as compatible, metabolic and counteracting cytoprotectants in high osmolarity and other stresses, J. Exp. Biol. 208 (2005) 2819–2830.
[18] P.H. Yancey, G.N. Somero, Methylamine osmoregulatory solutes of elasmobranch fishes counteract urea inhibition of enzymes, J. Exp. Zool. 212 (1980) 205–213.
[19] B.A. Seibel, P.J. Walsh, Trimethylamine oxide accumulation in marine animals: relationship to acylglycerol storage, J. Exp. Biol. 205 (2002) 297–306.
[20] P.H. Yancey, Water stress, osmolytes and proteins, Amer. Zool. 41 (2001) 699–709.
[21] A. Mukherjee, M.K. Santra, T.K. Beuria, D. Panda, A natural osmolyte trimethylamine N-oxide promotes assembly and bundling of the bacterial cell division protein, FtsZ and counteracts the denaturing effects of urea, FEBS J. 272 (2005) 2760–2772.
[22] D.L. Sackett, Natural osmolyte trimethylamine N-oxide stimulates tubulin polymerization and reverses urea inhibition, Am. J. Physiol. 273 (1997) R669–R676.

[23] D.-S. Yang, C.M. Yip, T.H.J. Huang, A. Chakrabartty, P.E. Fraser, Manipulating the amyloid-β aggregation pathway with chemical chaperones, J. Biol. Chem. 274 (1999) 32970–32974.
[24] N.A. Chebotareva, S.E. Harding, D.J. Winzor, Ultracentrifugal studies of the effect of molecular crowding by trimethylamine N-oxide on the self-association of muscle glycogen phosphorylase *b*, Eur. J. Biochem. 268 (2001) 506–513.
[25] T.Y. Lin, S.N. Timasheff, Why do some organisms use a urea–methylamine mixture as osmolyte? Thermodynamic compensation of urea and trimethylamine N-oxide interactions with protein, Biochemistry 33 (1994) 12695–12701.
[26] Y. Qu, D.W. Bolen, Hydrogen exchange kinetics of RNase A and the urea: TMAO paradigm, Biochemistry 36 (2003) 9101–9108.
[27] P. Singh, I. Haque, F. Ahmad, Counteracting osmolytes trimethylamine N-oxide destabilizes proteins at pH below its pK_a, J. Biol. Chem. 280 (2005) 11035–11042.
[28] P.R. Wills, D.J. Winzor, Thermodynamic analysis of "preferential solvation" in protein solutions, Biopolymers 33 (1993) 1627–1629.
[29] P.R. Wills, W.D. Comper, D.J. Winzor, Thermodynamic nonideality in macromolecular solutions: interpretation of virial coefficients, Arch. Biochem. Biophys. 300 (1993) 206–212.
[30] C.L. Winzor, D.J. Winzor, L.G. Paleg, G.P. Jones, B.P. Naidu, Rationalization of the effect of compatible solutes on protein stability in terms of thermodynamic nonidiality, Arch. Biochem. Biophys. 296 (1992) 102–107.
[31] P.R. Davis-Searles, A.J. Saunders, D.A. Erie, D.J. Winzor, G.J. Pielak, Interpreting the effects of small uncharged solutes on protein-folding equilibria, Annu. Rev. Biophys. Biomol. Struct. 30 (2001) 271–306.
[32] D.J. Winzor, P.R. Wills, Thermodynamic nonideality of enzyme-solutions supplemented with inert solutes: yeast hexokinase revisited, Biophys. Chem. 57 (1995) 103–110.
[33] J. Poon, M. Bailey, D.J. Winzor, B.E. Davidson, W.H. Sawyer, Effects of molecular crowding on the interaction between DNA and the *Escherichia coli* regulatory protein TyrR, Biophys. J. 73 (1997) 3257–3264.
[34] C.N. Patel, S.M. Noble, G.T. Weatherly, A. Tripathy, D.J. Winzor, G.J. Pielak, Effect of molecular crowding by saccharides on α-chymotrypsin dimerization, Protein Sci. 11 (2002) 997–1003.
[35] M.P. Jacobsen, P.R. Wills, D.J. Winzor, Thermodynamic analysis of the effects of small inert cosolutes in the ultracentrifugation of noninteracting proteins, Biochemistry 35 (1996) 13173–13179.
[36] T.G.A. Lonhienne, D.J. Winzor, Interpretation of the reversible inhibition of adenosine deaminase by small cosolutes in terms of molecular crowding, Biochemistry 40 (2001) 9618–9622.
[37] T.G.A. Lonhienne, D.J. Winzor, Calorimetric demonstration of the potential of molecular crowding to emulate the effect of an allosteric activator on pyruvate kinase kinetics, Biochemistry 41 (2002) 6897–6901.
[38] D.R. Hall, M.P. Jacobsen, D.J. Winzor, Stabilizing effect of sucrose against irreversible denaturation of rabbit muscle lactate dehydrogenase, Biophys. Chem. 57 (1995) 47–54.
[39] P.R. Wills, D.R. Hall, D.J. Winzor, Interpretation of thermodynamic nonideality in sedimentation equilibrium experiments on proteins, Biophys. Chem. 84 (2000) 217–225.
[40] I.V. Baskakov, D.W. Bolen, Time-dependent effects of trimethylamine-N-oxide/urea on lactate dehydrogenase activity: an unexplored dimension of the adaptation paradigm, Biophys. J. 74 (1998) 2658–2665.
[41] I.V. Baskakov, D.W. Bolen, Forcing thermodynamically unfolded proteins to fold, J. Biol. Chem. 273 (1998) 4831–4834.
[42] Y. Liu, D.W. Bolen, The peptide backbone plays a dominant role in protein stabilization by naturally occurring osmolytes, Biochemistry 34 (1995) 12884–12891.
[43] S.N. Timasheff, Protein hydration, thermodynamic binding, and preferential hydration, Biochemistry 41 (2002) 13473–13482.
[44] S.N. Timasheff, Protein-solvent preferential interactions, protein hydration, and the modulation of biochemical reactions by solvent components, Proc. Natl. Acad. Sci. U. S. A. 99 (2002) 9721–9726.
[45] I.V. Baskakov, D.W. Bolen, Trimethylamine-N-oxide counteracts urea effects on rabbit muscle lactate dehydrogenase function: a test of the counteraction hypothesis, Biophys. J. 74 (1998) 2666–2673.
[46] Y. Qu, D.W. Bolen, Efficacy of macromolecular crowding in forcing proteins to fold, Biophys. Chem. 101 (2002) 155–165.
[47] N.A. Chebotareva, I.E. Andreeva, V.F. Makeeva, B.I. Kurganov, N.B. Livanova, S.E. Harding, Self-association of phosphorylase kinase from rabbit skeletal muscle in the presence of natural osmolyte, trimethylamine N-oxide, Progr. Colloid Polym. Sci. 119 (2002) 70–76.
[48] N.A. Chebotareva, A.V. Meremyanin, V.F. Makeeva, B.I. Kurganov, Self-association of phosphorylase kinase under molecular crowding conditions, Progr. Colloid Polym. Sci. 131 (2006) 83–92.
[49] N.A. Chebotareva, I.E. Andreeva, V.F. Makeeva, N.B. Livanova, B.I. Kurganov, Effect of molecular crowding on self-association of phosphorylase kinase and its interaction with phosphorylase *b* and glycogen, J. Mol. Recognit. 17 (2004) 426–432.
[50] V.E. Morozov, T.B. Eronina, I.E. Andreeva, G.V. Silonova, N.V. Soloviyova, E.I. Schors, N.B. Livanova, B.F. Poglazov, Purification, quaternary structure and regulatory properties of phosphorylase kinase from pigeon skeletal muscle, Biokhimiya 54 (1989) 448–455 (in Russian).
[51] U.K. Laemmli, Cleavage of structural proteins during the assembly of the head of bacteriofage T_4, Nature 227 (1970) 680–685.
[52] International Standard ISO 13321:1996(E). Particle size analysis — Photon correlation spectroscopy, International Organization for Standardization, Geneve, Switzerland, 1996.
[53] P.H. Brown, A. Balbo, P. Schuck, Using prior knowledge in the determination of macromolecular size-distributions by analytical ultracentrifugation, Biomacromolecules 8 (2007) 2011–2024.
[54] P.H. Brown, P. Schuck, Macromolecular size-and-shape distributions by sedimentation velocity analytical ultracentrifugation, Biophys. J. 90 (2006) 4651–4661.
[55] C.H. Chervenka, A manual of methods for the analytical ultracentrifuge, Spinco Division of Beckman Instruments Inc., Palo Alto, CA, 1969.
[56] A.P. Minton, Implications of macromolecular crowding for protein assembly, Curr. Opinion Struct. Biol. 10 (2000) 34–39.
[57] V.F. Makeeva, N.A. Chebotareva, I.E. Andreeva, N.B. Livanova, B.I. Kurganov, Interaction of phosphorylase kinase from rabbit skeletal muscle with flavin adenin dinucleotide, Biochemistry (Moscow) 71 (2006) 808–814.
[58] A.V. Meremyanin, T.B. Eronina, N.A. Chebotareva, S.Yu. Kleimenov, I.K. Yudin, K.O. Muranov, M.A. Ostrovsky, B.I. Kurganov, Effect of α-crystallin on thermal aggregation of glycogen phosphorylase *b* from rabbit skeletal muscle, Biochemistry (Moscow) 72 (2007) 7518–7528.
[59] H.A. Khanova, K.A. Markossian, B.I. Kurganov, A.M. Samoilov, S.Yu. Kleimenov, D.I. Levitsky, I.K. Yudin, A.C. Timofeeva, K.O. Muranov, M. A. Ostrovsky, Mechanism of chaperone-like activity. Suppression of thermal aggregation of β_L-crystallin by α−crystallin, Biochemistry 44 (2005) 15480–15487.
[60] K.A. Markossian, H.A. Khanova, S.Y. Kleimenov, D.I. Levitsky, N.A. Chebotareva, R.A. Asryants, V.I. Muronetz, L. Saso, I.K. Yudin, B.I. Kurganov, Mechanism of thermal aggregation of rabbit muscle glyceraldehyde-3-phosphate dehydrogenase, Biochemistry 45 (2006) 13375–13384.
[61] K.A. Markossian, B.I. Kurganov, D.I. Levitsky, H.A. Khanova, N.A. Chebotareva, A.M. Samoilov, T.B. Eronina, N.V. Fedurkina, L.G. Mitskevich, A.V. Merem'yanin, S.Yu. Kleymenov, V.F. Makeeva, V.I. Muronets, I.N. Naletova, I.N. Shalova, R.A. Asryants, E.V. Schmalhausen, L. Saso, Yu.V. Panyukov, E.N. Dobrov, I.K. Yudin, A.C. Timofeeva, K.O. Muranov, M.A. Ostrovsky, Mechanisms of chaperone-like activity, in: T.R. Obalinsky (Ed.), Protein Folding: New Research, Nova Science Publishers Inc., New York, 2006, pp. 89–171.
[62] N. Golub, A. Meremyanin, K. Markossian, T. Eronina, N. Chebotareva, R. Asryants, V. Muronets, B. Kurganov, Evidence for the formation of start aggregates as an initial stage of protein aggregation, FEBS Letters 581 (2007) 4223–4227.
[63] M. Elimelech, J. Gregory, X. Jia, R.A. Williams, Particle Deposition and Aggregation: Measurement, Modelling and Simulation, Butterworth-Heinemann Ltd., Boston, 1995.
[64] R. Jullien, R. Botet, Aggregation and Fractal Aggregates, World Scientific Publishing Co. Pte. Ltd., Singapore, 1987.
[65] D.A. Weitz, J.S. Huang, M.Y. Lin, J. Sung, Limits of the fractal dimension for irreversible kinetic aggregation of gold colloids, Phys. Rev. Lett. 54 (1985) 1416–1419.

[66] D. Weitz, M. Lin, Dynamic scaling of cluster-mass distributions in kinetic colloid aggregation, Phys. Rev. Lett. 57 (1986) 2037–2040.
[67] M. Lin, H. Linsday, D. Weitz, R. Ball, R. Klein, P. Meakin, Universality of fractal aggregates as probed by light scattering, Proc. R. Soc. Lond. A 423 (1989) 71–87.
[68] M. Berka, J.A. Rice, Relation between aggregation kinetics and the structure of kaolinite aggregates, Langmuir 21 (2005) 1223–1229.
[69] D. Winklmair, A simple approach to the theory of cooperative aggregation of biological macromolecules, Arch. Biochem. Biophys. 147 (1971) 509–514.
[70] J. Engel, D. Winklmair, Cooperative association, in: R. Jaenicke, E. Helmreich (Eds.), Protein–Protein Interactions, Springer-Verlag, Berlin, 1972, pp. 159–181.
[71] S. Keresztes-Nagy, M.H. Klapper, L. Lazer, I.M. Klotz, Hybridization experiments: evidence of dissociation equilibrium in hemerythrin, Science 150 (1965) 357–379.
[72] L.W. Nichol, W.J. Jackson, D.J. Winzor, A theoretical study of the binding of small molecules to a polymerizing protein system. A model for allosteric effects, Biochemistry 6 (1967) 2449–2456.
[73] J.C. Thomes, J. Archambault De Vençay, R. Julien, New relations for activity analysis of associating enzymes, Biochem. J. 185 (1980) 339–347.
[74] B.I. Kurganov, Allosteric enzymes, Kinetic Behaviour, John Wiley & Sons, Chichester, 1982, p. 243.
[75] S. Sprang, R. Fletterick, M. Stern, D. Yang, N. Madsen, J. Sturtevant, Analysis of an allosteric binding site: the nucleoside inhibitor site of phosphorylase, Biochemistry 21 (1982) 2036–2048.
[76] N.A. Chebotareva, S.V. Klinov, B.I. Kurganov, Regulation of muscle glycogen phosphorylase by physiological effectors, Biotechnol. Genet. Eng. Rev. 18 (2001) 265–297.
[77] S.Yu. Sundukov, G.A. Solovyeva, Interaction of glycogen synthase of rabbit skeletal muscles with flavin mononucleotide, Biokhimiya 54 (1989) 1478–1484 (Russian).